Ceramics International 42 (2016) 17466–17471

Contents lists available at ScienceDirect

Ceramics International

journal homepage: www.elsevier.com/locate/ceramint

Comparative study of oxide and non-oxide additives in high thermal conductive and high strength Si_3N_4 ceramics

Hyun Min Lee [a], Eun Bok Lee [b], Dong Lae Kim [b], Do Kyung Kim [a,*]

[a] Department of Materials Science and Engineering, Korea Advanced Institute of Science and Technology (KAIST), 291 Daehak-ro, Yuseong-gu, Daejeon, 34141 Republic of Korea

[b] Advanced Materials R&D Department, KCC Corporation, 19 Wanjusandan 4-ro, Wanju-gun, Jeonbuk-do, 55321 Republic of Korea

ARTICLE INFO

Article history:
Received 13 May 2016
Received in revised form
8 August 2016
Accepted 8 August 2016
Available online 19 August 2016

Keywords:
Si_3N_4
Non-oxide additives
Thermal conductivity
Flexural strength
Microstructure

ABSTRACT

A comparative study between oxide and non-oxide sintering additive was conducted to examine the thermal and mechanical properties of Si_3N_4 ceramics. The effects of additive types (oxide or non-oxide) on microstructure, thermal conductivity and mechanical strength were investigated. Replacement of oxide additives by non-oxide additives induced a decrease in the secondary phase and lattice oxygen contents of sintered samples. The use of non-oxide sintering additives increased the thermal conductivity of Si_3N_4 ceramics; however, the sintering additive had less impact on the ceramic flexural strength. The measured strengths of all samples ranged from 822 MPa to 916 MPa. Therefore, the thermal conductivity of ceramics incorporating non-oxide sintering additives increased while maintaining flexural strength; these materials possessed a flexural strength of 862 MPa and a thermal conductivity of 101.5 W/mK.

1. Introduction

Recently, power electrical device technology is moving toward higher voltage, larger current, greater power density, and smaller size. Power electronic devices have been widely used for various applications, such as transportation and industrial robots. This movement requires innovative technologies beyond Si semiconductors; the development of wide-band gap semiconductors, such as SiC and Ga_2O_3 [1,2]. However, a high power density will induce large thermal stresses in devices, which will lead to greater stresses being placed on the brittle ceramic substrates that function as electrical insulation. Therefore, the development of a ceramic substrate that possesses high reliability and thermal conductivity is necessary.

A great deal of research has investigated the development of ceramics with high thermal conductivity. To date, aluminum nitride (AlN) ceramics have been used as a major ceramic substrate material for power electronic devices because it possesses a high thermal conductivity (estimated value of intrinsic thermal conductivity is 320 W/mk) [3,4]. However, AlN ceramic substrates suffer from shorter lifetimes due to the lack of mechanical properties, such as a bending strength of 300–400 MPa [5]. Although several research groups have focused on enhancing the strength of AlN ceramics, there were limitations to their use as a structural substrate material due to their low mechanical strength and toughness [6–8].

Silicon nitride (Si_3N_4) ceramics have been investigated for high temperature structural applications, and their usage is expanding toward various applications including power electronics. Haggerty and Lightfoot calculated that the intrinsic thermal conductivity of Si_3N_4 ceramics could be as high as 200–320 W/mK at room temperature [9,10]. However, the reported thermal conductivity values of Si_3N_4 ceramics have been much lower than this intrinsic value. The thermal conductivity in Si_3N_4 ceramics are influenced by various factors. One is the nature of the material itself. Si_3N_4 possesses very strong covalent bonding between the Si and N atoms resulting in poor sinterability [11–14]. Dense Si_3N_4 ceramics generally can be obtained by liquid phase sintering processes. The addition of sintering additives is essential to fabricate dense Si_3N_4; however, a residual grain boundary phase (secondary phase) remains. Because the secondary phases have very low thermal conductivity (less than 5 W/mK), their existence causes a reduction of the thermal conductivity [15–17]. In addition to this secondary phase, lattice defects within the Si_3N_4 grains are also known to affect the thermal conductivity. Heat is transmitted only by phonons because ceramics have no free electrons. The existence of lattice defects induces phonon scattering and reduces the thermal conductivity. Oxygen-related defects have a significant impact on the thermal conductivity of Si_3N_4 ceramics. An oxide layer, SiO_2, always exists on the surface of Si_3N_4 particles, and

* Corresponding author.
E-mail address: dkkim@kaist.ac.kr (D.K. Kim).

http://dx.doi.org/10.1016/j.ceramint.2016.08.051
0272-8842/

Si_3N_4 ceramics usually require the addition of an oxide as a sintering additive in order to form, at the relevant eutectic point, a liquid phase and promote densification. However, oxygen content is one of the major factors in reducing the thermal conductivity of Si_3N_4 ceramics. Kitayama et. Al. found that the thermal conductivity increases as the oxygen content in the Si_3N_4 grain decreases. When oxygen impurities are dissolved in a lattice, they generated silicon vacancies and caused phonon scattering [18,19].

Therefore, it is important to determine the factors that specifically influence the thermal conductivity of Si_3N_4 ceramics. A possible approach to improving the thermal conductivity of Si_3N_4 ceramics with a minimum deterioration of the mechanical strength is to fully understand the impact of each factor and to find the appropriate combinations of factors.

In an effort to improve the thermal conductivities of silicon nitride ceramics, we attempted to prepare dense Si_3N_4 ceramics and determine the effects of different sintering agents on these Si_3N_4 ceramics. Two different types of sintering additives, oxide and non-oxide additives, were selected and the properties of their corresponding ceramics were compared. $MgSiN_2$, which was synthesized using a nitridation process, was used instead of MgO, and rare-earth oxides (Y_2O_3, and Yb_2O_3) were replaced by rare-earth fluoride additives (YF_3, and YbF_3). Fluoride additives have high vapor pressures at high temperature; therefore, a degree of evaporation is expected upon complete densification at high temperature, and these materials are expected to retain less of a grain boundary phase and to improve the thermal conductivity.

2. Experimental procedure

2.1. Powder preparations

High-purity commercial powders were used for fabricating all specimens to reduce the effects of impurities. Green Si_3N_4 was prepared using commercially available α-Si_3N_4 (E-10 grade, Ube Industries, Ube, Japan). Oxide sintering additives - MgO (Aldrich Chemicals Co., Milwaukee, WI), Y_2O_3 (Aldrich Chemicals Co., Milwaukee, WI), and Yb_2O_3 (Aldrich Chemicals Co., Milwaukee, WI), and non-oxide additives - $MgSiN_2$ (prepared by the nitridation of Mg_2Si in our laboratory), YF_3 (Aldrich Chemicals Co., Milwaukee, WI), and YbF_3 (Aldrich Chemicals Co., Milwaukee, WI) were selected for each of the compositions; these compositions are shown in Table 1. The sintering additive, $MgSiN_2$ was synthesized by direct nitridation of Mg_2Si powder (Aldrich Chemicals Co., Milwaukee, WI). The Mg_2Si powder was placed in a BN crucible and the crucible was placed inside a graphite crucible and graphite furnace (Astro Thermal Technology, Santa Barbara, CA). Nitridation was performed at a temperature 1400 °C with a hold time of 1 h under flowing nitrogen gas condition [20].

Si_3N_4 powder was mixed with sintering additives by a ball milling process in a polyethylene bottle for 24 h. High purity 2-propanol and Si_3N_4 balls were used as the medium. The mixture was dried on a hot plate with stirring. The dried powder was sieved though a 200-mesh sieve and shaped into a 40 mm diameter disk under a pressure of 30 kg fcm^{-2}. The pellet was then isostatically cold-pressed (CIP) at a pressure of 200 MPa. The CIPed specimens (green products) were placed in the graphite crucible with a powder bed mixture of 1:1 for Si_3N_4/BN. Hot-pressing (Astro Thermal Technology, Santa Barbara, CA), was conducted at 1800 °C for 2 h; next, sample was post heat treated at 1850 °C for 3 h. The heating rate during sintering was 10 °C/min, and the cooling rate was 25 °C/min.

2.2. Characterization methods

Bulk density was measured by Archimedes' method using distilled water as the medium; the theoretical density was calculated using the composite mixture. X-ray diffractometry (XRD, Rigaku, D/MAX-IIIC, Tokyo, Japan) was used to identify the phase compositions. The microstructure was characterized by scanning electron microscopy (FE-SEM; Philips XL30 FEG, Eindhoven, Netherlands).

The thermal conductivity of the sintered materials was measured by laser flash method with a glass-Nd laser and an InSb infrared sensor using a Xenon Flash instrument (LFA 447 Nanoflash, Netzsch Instruments Inc., Burlington, MA, USA). The maximum output of the laser beam was 15 J/pulse and the exposure time was 0.4 ms. The size of the measured specimen was 12.7 mm in diameter and 2 mm in thickness. The bulk thermal conductivity was calculated to multiply measured thermal diffusivity by apparent density and heat capacity measured by DSC (Differential Scanning Calorimeter). The precision of this apparatus was estimated to be ±3%. Each reported thermal conductivity was an average of three measurements.

The sintered body was ground for 30 min using a high energy mill and screened through a 500 mesh sieve (to remove coarse particles). To remove the grain boundary phase and possible metal compounds, the powder was treated first with 50% HF at 60 °C for 3 h and then, with 50% H_2SO_4 at 120 °C for 2 h. The slurry was washed with distilled water until it reached a pH value of 7. Each powder was dried at 120 °C for 10 h and passed through a 100 mesh sieve. A commercial hot-gas extraction analyzer (OHN-2000, Lab&Part Incheon, Korea) was used for lattice oxygen content determination.

For the measurement of the flexural strength, the sintered disks were cut into bars. The rectangular bars with dimensions of 3.0 mm × 4.0 mm × 35 mm were tested using a 20 mm support span and a crosshead speed of 0.5 mm/min. The bars were polished with 6 and 1 μm diamond paste in an alcohol-based slurry (Blue Lube, Struers) and edges were beveled for three-point bending strength test. The reported flexural strength is an average of five tests.

3. Results and discussion

3.1. Synthesis of $MgSiN_2$ powder

Fig. 1 shows the resulting phase after nitridation. The $MgSiN_2$ phase was identified by XRD analysis. These results indicate that the $MgSiN_2$ phase was successfully synthesized along with free

Table 1
Compositions of the starting powder.

(vol. %)

Sample	MgO	$MgSiN_2$	Y_2O_3	YF_3	Sample	MgO	$MgSiN_2$	Yb_2O_3	YbF_3
MOYO	5		2		MOYbO	5		2	
MNYO		5	2		MNYbO		5	2	
MNYF		5		2	MNYbF		5		2

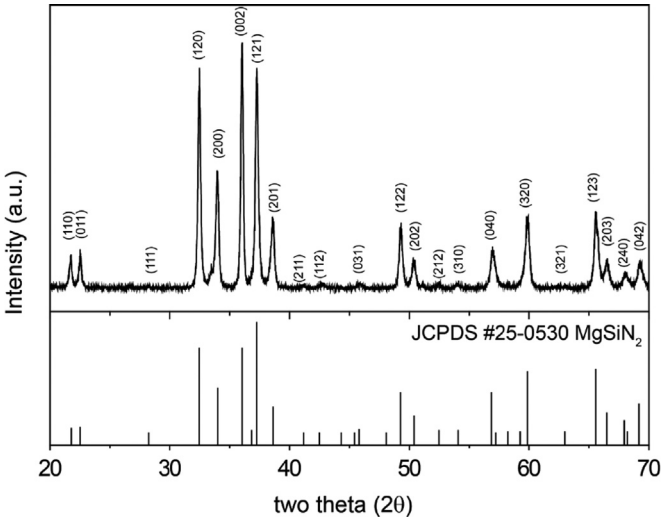

Fig. 1. XRD results of $MgSiN_2$ phase prepared by nitridation of Mg_2Si.

$MgSi_2$, Si and MgO phases. The simple nitridation process is demonstrated to follow the following reaction [20]:

$$Mg_2Si + N_2 \rightarrow MgSiN_2 + Mg \uparrow \quad (1)$$

Many studies have determined the effect of $MgSiN_2$ sintering additives on the thermal conductivity of Si_3N_4. Replacing MgO with $MgSiN_2$ as a sintering additive induces a high nitrogen/oxygen ratio of the liquid phase during sintering [21–23].

3.2. Sintering of Si_3N_4 ceramics

Si_3N_4 ceramics with sintering additives were hot-pressed at 1800 °C for 2 h under 25 MPa of pressure and continually post heat treated at 1830 °C for 4 h. All compositions reach a density of 3.20 g cm^{-3}, resulting in a relative density $>97\%$ of the theoretical value. Fig. 2 shows the XRD results for the sintered materials. The α-Si_3N_4 phase was not detected in any of the sintered samples, which means that the α-to-β phase transformation was completed during sintering. Table 2 represents the crystalline secondary phases present in the sintered samples. The $RE_4Si_2N_2O_7$ (RE = Y or Yb) phase was observed in the samples that had oxide additives. Conversely, no crystalline phases were detected for the magnesium compounds in any of samples. The secondary phases were influenced by the types of sintering additive. The insert images in Fig. 2 provide the magnified views of the XRD peaks of the secondary phases. The intensity of the secondary phases decreased with the replacement of the oxide additives by non-oxide additives. The medium intensity of the XRD peaks became very weak in the samples MNYO and MNYbO, and finally, no trace of a secondary phase was observed in samples MNYF and MNYbF (Fig. 2). The non-oxide additives induced high ratios of nitrogen/oxygen in the liquid phase which leads to an increase of viscosity in the liquid phase during the sintering. Thus, the remaining amount of secondary phase decreased.

Fig. 3 shows the microstructure of the polished and plasma etched surface of the sintered samples. For the plasma etched surface, the bright area represents the secondary phases. The amounts of secondary phases were also visibly reduced via the replacement of oxides with non-oxide additives, while no significant grain growth was observed. Although samples MOYO and MOYbO contained both thick film at the boundary phases and isolated grain boundary pockets (Fig. 3(a) and (d)), samples MNYF and MNYbF had very thin secondary phases (Fig. 3(c) and (f)). Furthermore, some traces of evaporation of secondary phases at

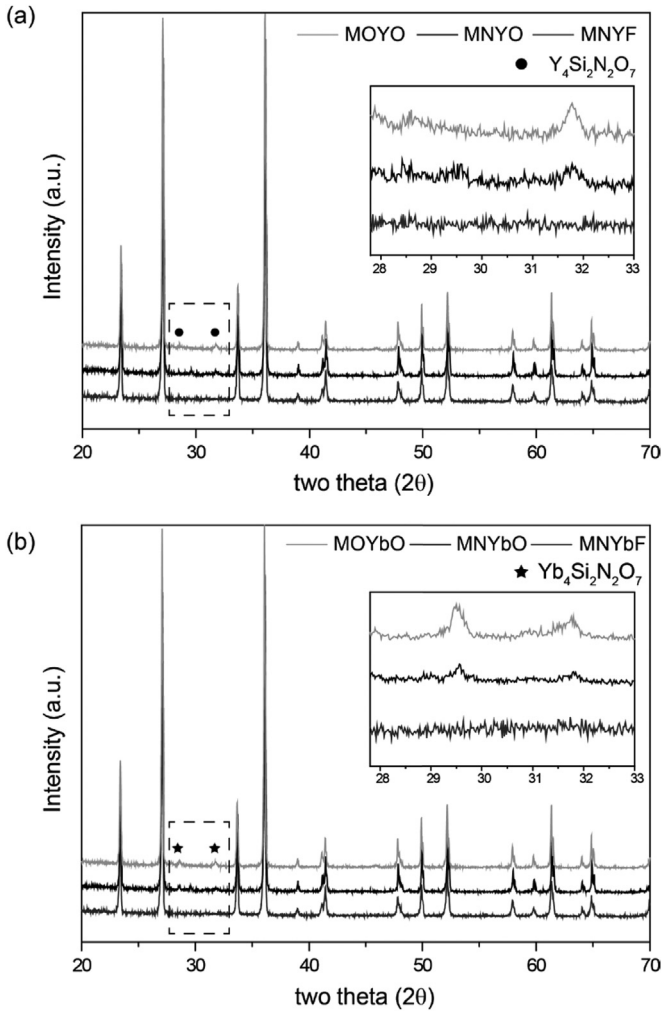

Fig. 2. XRD results of (a) Y-composition and (b) Yb-compositions added Si_3N_4.

Table 2
Crystalline secondary phase present in the sintered Si_3N_4 ceramics identified by XRD.

Sample	Secondary phase	Sample	Secondary phase
MOYO	$Y_4Si_2N_2O_7$ (m)	MOYbO	$Yb_4Si_2N_2O_7$ (m)
MNYO	$Y_4Si_2N_2O_7$ (vw)	MNYbO	$Yb_4Si_2N_2O_7$ (vw)
MNYF	No trace of secondary phase	MNYbF	No trace of secondary phase

*m = medium, vw = very weak.

the grain boundary areas were observed in the non-oxide added samples. All samples went through hot-pressing and post heat treatment processes. Because of the high vapor pressure of the non-oxide additives, the secondary phase composed of non-oxide additives might have evaporated during the high temperature heat treatment.

3.3. Thermal and mechanical properties

The thermal conductivity values of the hot-pressed Si_3N_4 samples with different sintering additives are presented in Fig. 4. Samples with Yb-additives (MOYbO, MNYbO, and MNYbF) show higher values of thermal conductivity than those with yttrium additives (MOYO, MNYO, and MNYF). The effects of rare-earth elements on the properties of Si_3N_4 ceramics have been reported by several research groups. Kitayama, et.al. [24] reported that the thermal conductivity of Si_3N_4 ceramics increased with decreasing

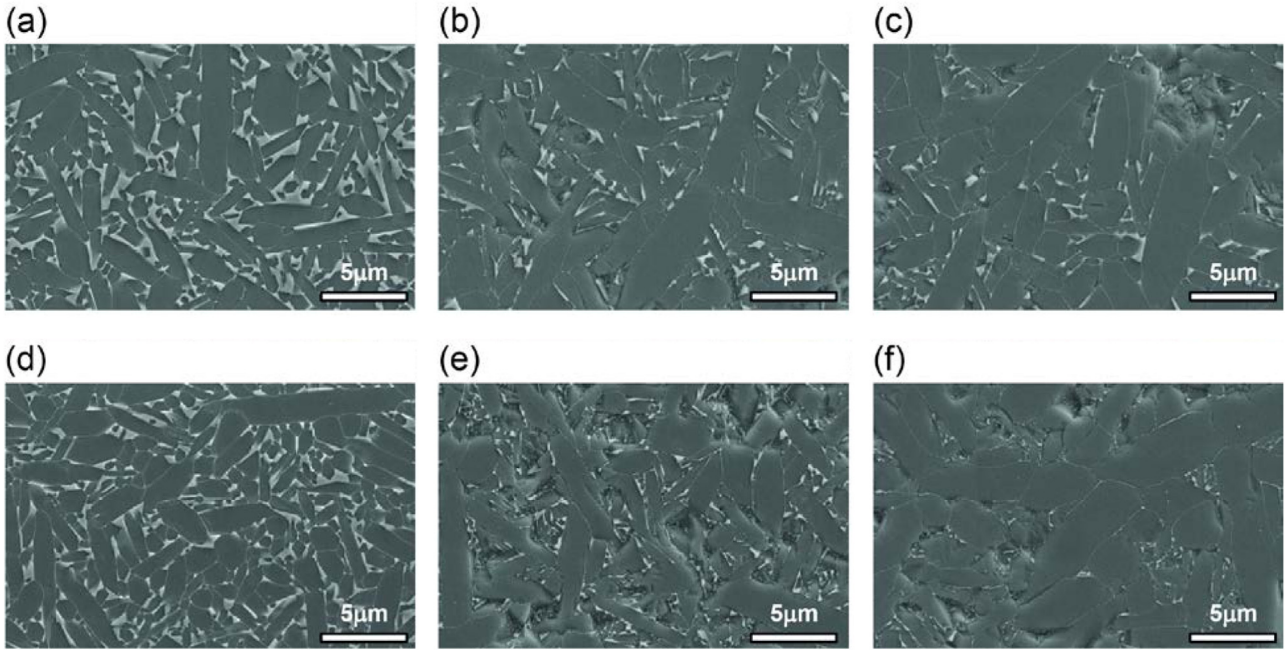

Fig. 3. Microstructure of polished and plasma-etched surface of oxide additives (a) sample MOYO and (d) MOYbO; mixed additives (b) MNYO and (e) MNYbO; non-oxide additives (c) MNYF and (f) MNYbF. The amount of residual secondary phase decreased as oxide additives were replaced by non-oxide ones. All images have the same magnification.

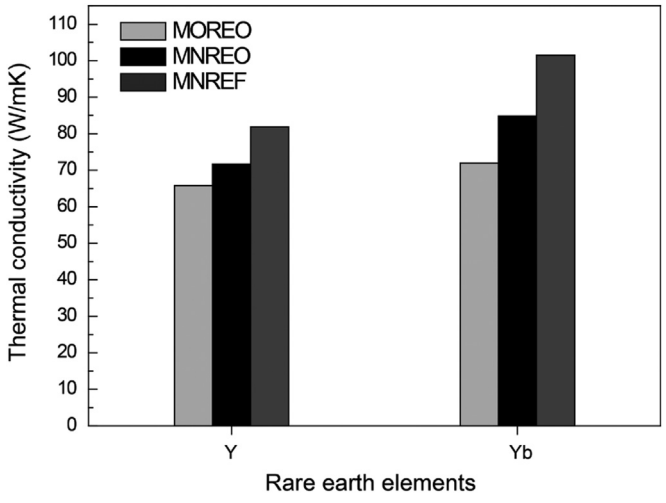

Fig. 4. Thermal conductivities of Si_3N_4 ceramics. Thermal conductivity increased with non-oxide additives and Yb-compounds added sample shows higher thermal conductivity than Y-compounds added sample.

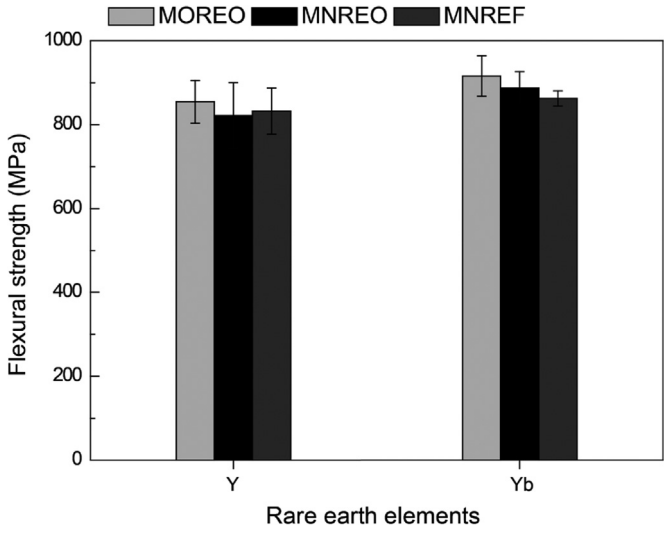

Fig. 5. Flexural strength of Si_3N_4 ceramics. Types of sintering additives (oxide or non-oxide) has less affected on the strength. Yb-elements added Si_3N_4 ceramics showed higher strength than one of Y-elements added samples.

ionic radius of added rare-earth elements. Therefore, our thermal conductivity results for Y and Yb-elements added samples match well with the results of Kitayama. The type of sintering additive, in addition to the type of rare-earth element, also affected the thermal conductivity. Thermal conductivity increased as oxide additives were replaced by non-oxide ones. Samples with only non-oxide additives (MNYF and MNYbF) showed the highest values of thermal conductivity (81.8 and 101.5 W/mK, respectively) and samples with mixed types of additives (MNYO and MNYbO) followed with thermal conductivity values of 71.7 and 84.9 W/mK, respectively. Both samples with only oxide additives (MOYO and MNYbO) had the lowest values of thermal conductivity (65.8 and 71.9 W/mK), respectively.

Investigations of the influence of additive types on the flexural strength were also conducted, and the measured strength values are presented in Fig. 5. In contrast to thermal conductivity, the strength behavior according to the type of sintering additives showed notably little correlation. All measured samples possessed flexural strength values between 822 and 916 MPa. Although all samples were subjected to the same sintering conditions, there was no significant grain growth observed. It was found that the flexural strength of MOYO was 854 MPa, but the strengths of samples MNYO and MNYF were 822 MPa and 832 MPa, respectively. The replacement of MgO by $MgSiN_2$ resulted in a slight decrease of flexural strength for the Y-element added samples, the replacement of Y_2O_3 by YF_3 induced an increase in the flexural strength. Conversely, the Yb-element added samples showed a decrease of the flexural strength as the oxides were replaced by non-oxide additives. The flexural strengths of MOYbO, MNYbO, and MNYbF were 916 MPa, 887 MPa, and 862 MPa, respectively.

To determine the effects of sintering additives, Fig. 6 illustrates

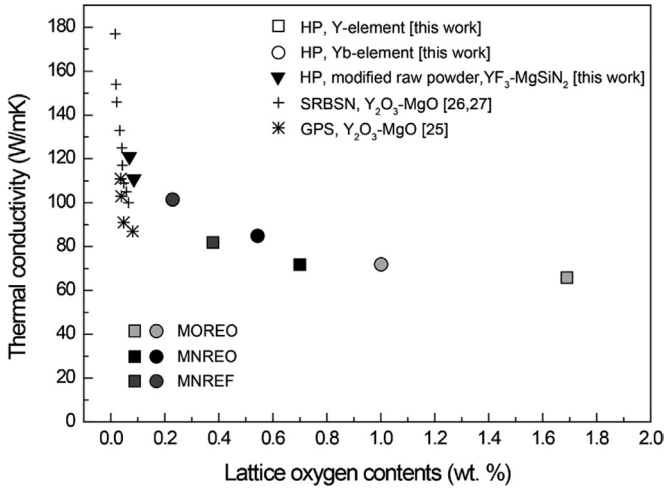

Fig. 6. The relationship between the lattice oxygen contents and the thermal conductivities for sintered Si_3N_4 ceramics.

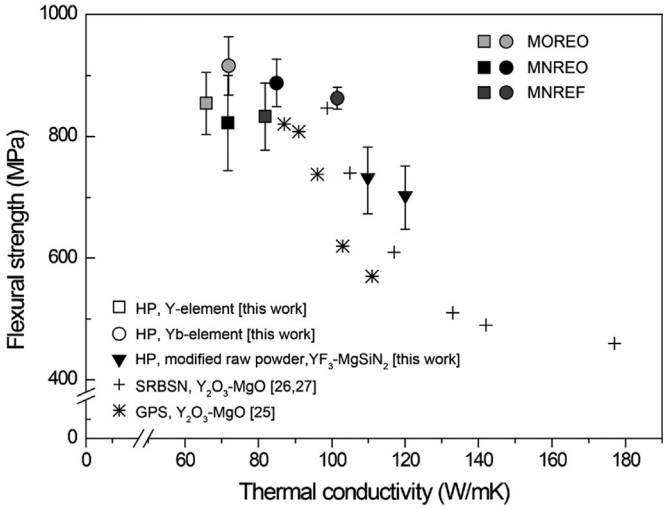

Fig. 7. The relation between thermal conductivity and flexural strength for the hot-pressed Si_3N_4 ceramics with sintering additives of Y or Yb-elements.

the relationship between thermal conductivity and the lattice oxygen content in sintered Si_3N_4 ceramics. Data on thermal conductivity and lattice oxygen content of Si_3N_4 ceramics from the different process conditions (GPS and SRBSN) were also added [25–27]. Despite the various sintering process methods, a close correlation is shown between them, obviously indicating that the thermal conductivity increases with decreasing lattice oxygen content. It has been shown that reducing the lattice oxygen content to less than 0.1% raises the thermal conductivity over 150 W/mK (Hirao and You Zhou reported 177 W/mK [17–19]). That research, however, involved conducting the annealing process for a prolonged period of time of over 60 h. This approach could make it possible to achieve a low lattice oxygen content and high thermal conductivity, but this prolonged annealing process caused significant coarsening of the grains, which led to a dramatic decrease in the mechanical strength (460 MPa) [25]. In the present work, the total oxygen content was high compared to those in the SRBSN or GPS methods, the hot-pressed Si_3N_4 ceramics presented moderately high value of thermal conductivities. The lattice oxygen content in the present work was decreased using non-oxide additives instead of oxide ones. For the different rare-earth elements Y and Yb, the hot-pressed Si_3N_4 might have different values of thermal conductivity even though the lattice oxygen contents were similar. In addition to the lattice oxygen content, the microstructural features were also influenced, including the grain size, the secondary phases and grain orientation [18,24]. However, the clear tendency shown in Fig. 6 is that the types of sintering additives worked as a crucial factor in governing the thermal conductivity of Si_3N_4 ceramics. We determined the effects of non-oxide additives on the thermal conductivity and these effects will probably increase even more if the lattice oxygen content can be reduced.

To reduce lattice oxygen defects further, we modified the raw Si_3N_4 powder. Commercially available α-Si_3N_4 powder (E-10 grade, Ube, Japan) was annealed in graphite crucible at 1500 °C under N_2 gas flowing for 10 h to reduce the presence of oxygen defects in the raw Si_3N_4 powder. It was found that the oxygen content decreased by 20% in the annealed Si_3N_4 powder (see Supplemental data). This affected the lattice oxygen content of the hot-pressed samples and thus led to an increase in the thermal conductivity. Hot-pressed samples with modified raw powder and sintering additives of YbF_3-$MgSiN_2$ had thermal conductivities of 109.9 W/mK and 120.1 W/mK after they were post heat treated at 1850 °C the sintering additive had less of an impact on could be obtained by reducing the lattice oxygen content by using modified raw powder and prolonging the sintering time.

The relationship between the thermal conductivity and the flexural strength of Si_3N_4 ceramics is plotted in Fig. 7. For comparison, data on the thermal conductivity and flexural strength of Si_3N_4 ceramics for different process conditions (GPS and SRBSN) were also included [25–27]. The samples containing the Yb-element additives showed higher flexural strength at any given level of thermal conductivity compared with those of the SRBSN or GPSed samples. A dramatic decrease of the flexural strength was observed for the SRBSN or GPSed samples; however, we were able to enhance the thermal conductivity with a minimum of deterioration of the flexural strength. Because we were able to reduce the oxygen content before the sintering process, which used the non-oxide additives and defect-reduced raw powder, it was possible to achieve a higher thermal conductivity within a short time of sintering, resulting in a finer microstructure and a higher flexural strength.

4. Conclusions

Dense Si_3N_4 ceramics were successfully fabricated by hot-pressing at 1800 °C for 2 h with different types of sintering additives, including MgO-Y_2O_3, $MgSiN_2$-Y_2O_3, $MgSiN_2$-YF_3, MgO-Yb_2O_3, $MgSiN_2$-Yb_2O_3, and $MgSiN_2$-YbF_3. The type of the sintering additive was observed to have a great effect on the microstructure, lattice oxygen content and thermal conductivity of Si_3N_4 ceramics. The use of non-oxide additives, such as $MgSiN_2$ and rare-earth fluorides (YF_3 or YbF_3), induced a decrease in the amount of secondary phases and lattice oxygen contents in the sintered samples. Thus, the thermal conductivity increases as non-oxide additives replace oxide ones. The thermal conductivity showed an increase from 65.8 to 81.8 W/mK in the samples with Y-element additives and an increase from 71.9 to 101.5 W/mK in the sample with Yb-element additives. In contrast, the sintering additive had less of an impact on the flexural strength of Si_3N_4 ceramics; this effect is attributed to fact that no significant grain growth was observed. All samples showed high flexural strength with values in a range of 822–916 MPa. The enhancement of the thermal conductivity is ascribed to the reduction of the secondary phase and the purification of defects (oxygen contents). A further increase of the thermal conductivity was achieved using a modified raw powder (oxygen content decreased from 1.27 wt% to 0.96 wt% via annealing process) and non-oxide additives. It was possible to reduce the

oxygen content before the sintering process, which used the non-oxide additives and defect-reduced raw powder, high thermal conductivity was achieved within a short time of sintering process. As a result, we were able to synthesize Si_3N_4 ceramics that had high thermal conductivity and high flexural strength.

Appendix A. Supporting information

Supplementary data associated with this article can be found in the online version at doi:10.1016/j.ceramint.2016.08.051.

References

[1] C.R. Eddy, D.K. Gaskill, Silicon carbide as a platform for power electronics, Science 324 (2009) 1398–1400.
[2] H. Juergensen, MOCVD technology in research, Dev. Mass Prod. Mater. Sci. Semicond. Proc. 4 (2001) 467–474.
[3] G.A. Slack, Nonmetallic crystals with high thermal-conductivity, J. Phys. Chem Solids 34 (1973) 321–335.
[4] G.A. Slack, R.A. Tanzilli, R.O. Pohl, J.W. Vandersande, The intrinsic thermal-conductivity of Aln, J. Phys. Chem Solids 48 (1987) 641–647.
[5] H.M. Lee, K. Bharathi, D.K. Kim, Processing and characterization of aluminum nitride ceramics for high thermal conductivity, Adv. Eng. Mater. 16 (2014) 655–669.
[6] H.M. Lee, D.K. Kim, High-strength AlN ceramics by low-temperature sintering with $CaZrO_3$-Y_2O_3 co-additives, J. Eur. Ceram. Soc. 34 (2014) 3627–3633.
[7] S. Wei, Z.P. Xie, W.J. Xue, Z.Z. Yi, J. Chen, L.X. Cheng, Fracture toughness of aluminum nitride ceramics at cryogenic temperatures, Ceram. Int. 40 (2014) 13715–13718.
[8] P. Xia, Z.H. Li, W.J. Wu, Y.M. Zhu, D.D. Feng, Effects of AlN on the thermal and mechanical properties of vitrified bond and vitrified CBN composites, Ceram. Int. 40 (2014) 12759–12764.
[9] K. Watari, High thermal conductivity non-oxide ceramics, J. Ceram. Soc. Jpn. 109 (2001) S7–S16.
[10] J.S. Haggerty, A. Lightfoot, Opportunities for enhancing the thermal conductivities of SiC and Si_3N_4 ceramics through improved processing, Ceram. Eng. Sci. Proc. 16 (2008) 475–487.
[11] G.R. Terwilliger, F.F. Lange, Pressureless sintering of Si_3N_4, J. Mater. Sci. 10 (1975) 1169–1174.
[12] W.D.G. Bocker, R. Hamminger, J. Heinrich, J. Huber, A. Roosen, Covalent hgh-performance ceramics, Adv. Mater. 4 (1992) 169–178.
[13] S.Q. Guo, N. Hirosaki, Y. Yamamoto, T. Nishimura, M. Mitomo, Hot-pressed silicon nitride ceramics with Lu_2O_3 additives: elastic moduli and fracture toughness, J. Eur. Ceram. Soc. 23 (2003) 537–545.
[14] B. Matovic, G. Rixecker, F. Aldinger, Pressureless sintering of silicon nitride with lithia and yttria, J. Eur. Ceram. Soc. 24 (2004) 3395–3398.
[15] H.J. Kleebe, M.J. Hoffmann, M. Ruhle, Influence of secondary phase chemistry on grain-boundary film thickness in silicon-nitride, Z. Met. 83 (1992) 610–617.
[16] M. Mitomo, S. Uenosono, Microstructural development during gas-pressure sintering of alpha-silicon nitride, J. Am. Ceram. Soc. 75 (1992) 103–108.
[17] T. Wasanapiarnpong, S. Wada, M. Imai, T. Yano, Effect of post-sintering heat-treatment on thermal and mechanical properties of Si_3N_4 ceramics sintered with different additives, J. Eur. Ceram. Soc. 26 (2006) 3467–3475.
[18] M. Kitayama, K. Hirao, M. Toriyama, S. Kanzaki, Thermal conductivity of b-Si_3N_4: I, effects of various microstructural factors, J. Am. Ceram. Soc. 82 (1999) 3105–3112.
[19] M. Kitayama, K. Hirao, A. Tsuge, K. Watari, M. Toriyama, S. Kanzaki, Thermal conductivity of b-Si_3N_4: II, effect of lattice oxygen, J. Am. Ceram. Soc. 83 (2000) 1985–1992.
[20] H. Uchida, K. Itatani, M. Aizawa, F.S. Howell, A. Kishioka, Synthesis of magnesium silicon nitride by the nitridation of powders in the magnesium-silicon system, J. Ceram. Soc. Jpn. 105 (1997) 934–939.
[21] H. Hayashi, K. Hirao, M. Toriyama, S. Kanzaki, K. Itatani, $MgSiN_2$ addition as a means of increasing the thermal conductivity of beta-silicon nitride, J. Am. Ceram. Soc. 84 (2001) 3060–3062.
[22] K. Hirao, H. Hayashi, K. Itatani, Y. Yamauchi, Effect of $MgSiN_2$ addition on microstructure and thermal conductivity of silicon nitride ceramics, Eur. Ceram. VII 206–2 (Pt 1-3) (2002) 1021–1024.
[23] Z.H. Liang, J. Li, L.C. Gui, G.H. Peng, Z. Zhang, G.J. Jiang, The role of $MgSiN_2$ during the sintering process of silicon nitride ceramic, Ceram. Int. 39 (2013) 3817–3822.
[24] M. Kitayama, K. Hirao, K. Watari, M. Toriyama, S. Kanzaki, Thermal conductivity of b-Si_3N_4: III, effect of rare-earth (RE = La, Nd, Cd, Y, Yb, and Sc) oxide additives, J. Am. Ceram. Soc. 84 (2001) 353–358.
[25] Y. Zhou, H. Hyuga, D. Kusano, Y. Yoshizawa, K. Hirao, A tough silicon nitride ceramic with high thermal conductivity, Adv. Mater. 23 (2011) 4563–4567.
[26] Y.Z. Kiyoshi Hirao, Hideki Hyuga, Tatsuki Ohji, Dai Kusano, High thermal conductivity silicon nitride ceramics, J. Korean Ceram. Soc. 49 (2012) 380–384.
[27] Y. Zhou, H. Hyuga, D. Kusano, Y.-i Yoshizawa, T. Ohji, K. Hirao, Development of high-thermal-conductivity silicon nitride ceramics, J. Asian Ceram. Soc. 3 (2015) 221–229.